aggregate packing as described by Olard (2015). The basis of the Binary Aggregate Packing (BAP) analysis is the triangle diagram describing the "Wall effect" and the "Loosening effect" concepts, which influence the potential for the interconnectedness of voids. The BAP concept allows for the zooming into the voids at each of the Micro, Midi and Macro levels of aggregate packing. To this end, the revised rational Bailey ratios have been formulated as ratio of the coarse/fine aggregate fraction instead of fine/coarse used in the traditional Bailey ratios, and are determined using Equations 6 to 8 respectively.

$$CA\,Ratio = \frac{(\%\,passing\,HS - \%\,passing\,PCS)}{100\% - \%\,passing\,HS} \quad \text{Equation 3}$$

$$FA_c\ \text{Ratio} = \frac{\%\ \text{Passing SCS}}{\%\ \text{Passing PCS}} \quad \text{Equation 4}$$

$$FA_f\ \text{Ratio} = \frac{\%\ \text{Passing TCS}}{\%\ \text{Passing SCS}} \quad \text{Equation 5}$$

$$CA_r = \frac{(\%100 - \%\text{HS})}{(\%\text{HS} - \%\text{PCS})} \quad \text{Equation 6}$$

$$\frac{C}{F} = \frac{(\%\text{NMPS} - \ \%\text{PCS})}{(\%\text{PCS})} \quad \text{Equation 7}$$

$$FA_{rmf} = \frac{(\%\text{SCS} - \%\text{TCS})}{(\%\text{TCS} - \%\text{Filler})} \quad \text{Equation 8}$$

HMA COMPACTABILITY

As defined before, compactability of HMA mix describes the energy needed to achieve a specific density or percentage air voids content. Over the years, serval approaches have been proposed to analyze HMA compaction data for particular compaction equipment to determine parameters that describe the compactability of HMA mixes (Bahia et al., 1998; Awed et al, 2015). Below is a list and brief description of the HMA compactability parameters that can be computed from a gyratory compactor basic output data. Figure 2 shows a graphical illustration of the compactability parameters.

- **Compaction energy index (CEI)** defined as the area under the densification curve from the 8th gyration to 92% compaction (Bahia et al., 1998), as illustrated in Figure 2a. HMA mixes with lower CEI values are desirably less difficult to compact.
- **Traffic densification index (TDI),** defined as the area under the densification curve from 92% to 98% compaction (Awed et al, 2015). It should be pointed out that in practice, certain mixes cannot easily be compacted to 98%. Therefore, a new traffic densification index was proposed. The new index is defined as the area under the densification curve from 92% to 300 gradations (i.e., **TDI_{300}**), as illustrated in Figure 2a. Generally, the smaller the TDI_{300}, the more difficult it is to compact the HMA mix.
- **Maximum shear stress (SS_{max}),** defined as the maximum shear stress during the gyratory compaction as illustrated in Figure 2b. Like TDI_{300}, this is also new parameter proposed in this study. The higher the SS_{max}, the more difficult it is to compact the HMA mix.
- **Area under the shear stress curve (ASS),** defined the area under shear stress from the 8th gyration to the maximum shear stress as illustrated in Figure 2b. This is also a new

parameter proposed in this study. Similar to SS_{max}, the higher the ASS, the more difficult it is to compact the HMA mix.

- **Compaction slope (CS),** which is the rate of compaction determined by using Equation 3 (Wang et al, 2000).

$$CS = \frac{\%compaction\ at\ N_{max} - \%compaction\ at\ N_{initial}}{\log(N_{max}) - \log(N_{initail})} \quad \text{Equation 9}$$

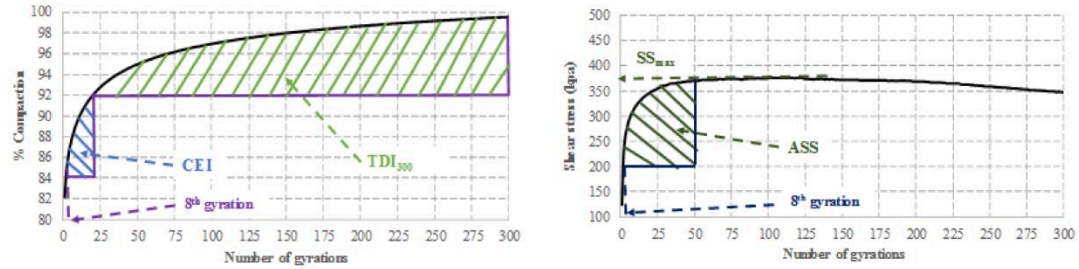

(a) CEI and TDI_{300} (b) SSmax and ASS

Figure 2. Conceptual Illustration of Compactability Parameters.

LABORATORY STUDY APPROACH

Aggregate and Asphalt Binder

Dolerite aggregates, which are routinely used in the production of HMA mixes, were sourced from a commercial asphalt plant in Gauteng province, South Africa. The aggregates consisted of 22.5 mm, 13.2 mm, 9.5 mm and 6.7 mm NMPS aggregate fractions, as well as crusher dust, mine sand and filler. Penetration-grade (35/50) asphalt-binder, which is equivalent to PG 64-16 as per the draft South African Performance Grade (PG) bitumen specification, was sourced from the same commercial asphalt plant. This binder, which conforms to the South African specification (SABS, 2016) was used to manufacture the HMA samples.

HMA Mix Design

The HMA mix design was also sourced from the same commercial asphalt plant in Gauteng province, South Africa. The HMA was a coarse-graded (stone-skeleton), with 20 mm NMPS, and is used routinely in the production of good-performing HMA mixes. The optimum asphalt-binder content was 4.3 %, and the design number of gyrations (N_{design}) is 125. In order to investigate the influence of aggregate gradation and packing characteristics on the compactability of HMA mixes, additional two gradation curves were designed. The gradation curves were designed to fall within the specified gradation envelopes according to the South African standard specifications for road and bridge works (COLTO, 1998) and resulting in three distinct coarser, medium, and finer gradation curves as illustrated in Figure 3.

HMA Mixing and Compaction

The mixing and compaction of the HMA specimens were done according to the South African Council for Scientific and Industrial Research (CSIR)'s test protocols for testing asphalt mixes in South Africa (Anochie-Boateng et al., 2010). The calculated masses of individual aggregate fractions were blended in accordance with the design gradation and pre-heated to the

required mixing temperature (160 °C). The required amount of pre-heated asphalt-binder and the pre-heated blended aggregate were placed into a pre-heated mechanical mixer, and mixed until a uniform mixture was obtained (approximately 15 minutes). After mixing, the loose HMA material was placed into an oven set at compaction temperature (145 C) for four hours to simulate short-term ageing. (Anochie-Boateng et al., 2010).

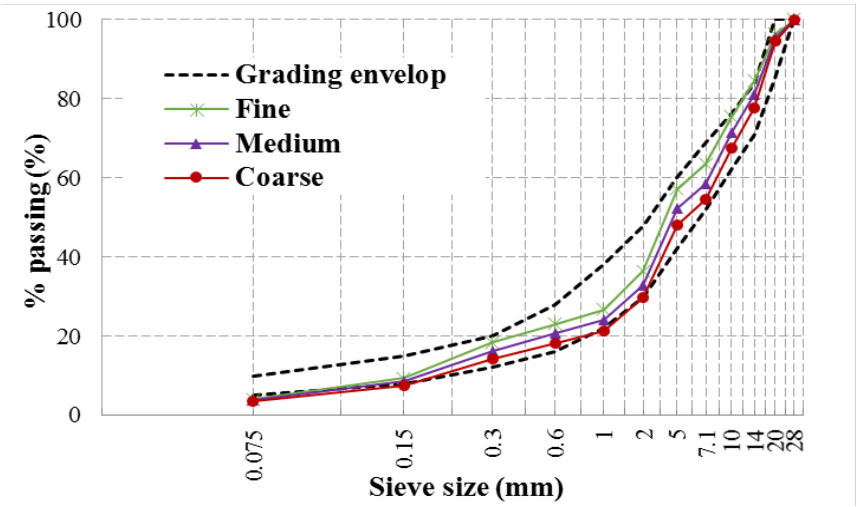

Figure 3. Aggregate gradation

Following the ageing simulation, HMA specimens were compacted using the SERVOPAC gyratory compactor. The mould diameter was 150 mm, and all the HMA specimens were compacted to 300 gyrations. For each of the three gradations, three replicates of HMA specimens were compacted. Figure 4a is a picture of the SERVOPAC gyratory compactor used in this study, with a typical compacted HMA specimen. Figures 4b and 4c show plots of the typical compaction output data (i.e., HMA specimen height and shear stress) from the SERVOPAC gyratory compactor, which are the basic used data for the analysis presented in this paper.

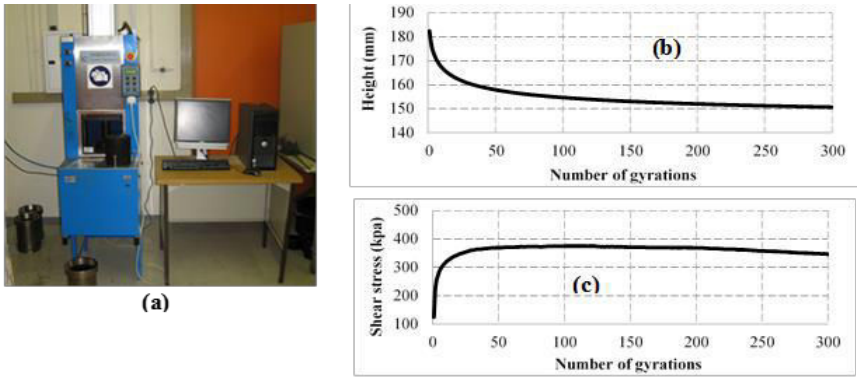

Figure 4. SERVOPAC gyratory compactor and typical output data.

Volumetric Analysis of Compacted HMA Specimens

The maximum void-less density (MVD) was determined on the loose HMA material according SANS 3001-AS11 (SABS, 2011a), whereas the bulk density (BD) of the compacted specimens was determined according to SANS 3001-AS10 (SABS, 2011b). Both the MVD and BD are key input data during the processing of the gyratory compaction data to determine the

compaction densification curve. The gyratory output data (i.e., specimen diameter and height after each gyration) was used to calculate the theoretical density, which was then used to determine the actual density after each gyration using Equation 10 (Anochie-Boateng et al., 2010).

$$Actual\ density = Calculated\ density \times \frac{Measured\ density}{Calculated\ density\ 300\ gyrations} \quad \text{Equation 10}$$

RESULTS AND DISCUSSIONS

Aggregate Gradation and Packing Parameters

Table 1 presents the aggregate gradation parameters and Bailey ratios for the three gradation structures investigated in this study. The coarser the aggregate gradation, the higher the G/S and *n* values, indicating that both, the G/S and *n* parameters can effectively differentiate the aggregate gradation structures. With respect to the traditional Bailey ratios, the results indicate that all the three ratios increase as the gradation structure becomes finer. Contrary to the traditional Bailey ratios, the revised rational ratios decrease as the aggregate gradation becomes finer. This trend was expected, as the revised rational ratios have been formulated in an inverse format (i.e., coarse/fine), in line with the binary aggregate fraction packing principles.

Table 1. Aggregate Gradation Parameters and Bailey Ratios.

	Gradation	*Aggregate Gradation Structure*		
	Parameter/Bailey ratio	*Coarse*	*Medium*	*Fine*
Gradation Parameters	*G/S*	1.29	1.12	1.01
	n	0.55	0.49	0.44
Traditional Bailey Ratios	*CA Ratio*	0.592	0.673	0.748
	FAc Ratio	0.442	0.460	0.468
	FAf Ratio	0.669	0.680	0.687
Revised Rational Bailey Ratios	CAr	1.688	1.487	1.336
	C/F	0.963	0.829	0.686
	FArmf	0.651	0.611	0.584

Parameters of HMA Compatability

Three replicates of HMA specimens were compacted for each of the three gradations, and the compaction data was analyzed to obtain five parameters (CEI, TDI_{300}, SS_{max}, ASS and CS) of HMA compactability. Sample statistics including mean, standard deviation (STD) and coefficient of variation (CoV) are included in the results presented in Table 2. With the exception of the ASS statistic, the CoV values are generally low (ranging from 0.5 to 14.9%), indicating that the measured compactability parameters are repeatable and exhibit low variability. In the subsequent section, the compactability parameters are correlated with aggregate packing parameters.

Parametric Correlations

The aggregate packing parameters were correlated with the average compactability parameters. Table 3 presents a summary of the correlation coefficient (r), as well as the coefficients of determination (R^2). The positive r values indicate a positive linear correlation or

relationship, whereas, negative r values indicate a negative linear correlation. Overall, the TDI_{300}, SS_{max}, ASS and CS parameters show stronger correlations with the aggregate gradation parameters and the Bailey ratios (r > |0.88|). However, the correlations for CEI were found to be relatively weaker to medium (r ranging from |0.53| to |0.72|).

Table 2. Summary of Parameters of HMA Compactability.

	Coarse			*Medium*			*Fine*		
Parameter	*Mean*	*STD*	*CoV(%)*	*Mean*	*STD*	*CoV(%)*	*Mean*	*STD*	*CoV(%)*
CEI	112	12.1	10.9	113	12.8	11.3	108	3.3	3.0
TDI300	1813	224.6	12.4	1866	277.9	14.9	2153	66.6	3.1
SSmax	389	2.1	0.5	382	7.0	1.8	369	5.5	1.5
ASS	396	93.8	21.1	328	21.8	5.6	309	43.7	23.3
CS	5.2	0.2	3.0	5.5	0.3	6.2	6.2	0.3	5.3

Table 3. Correlation Coefficients (R) and Coefficients of Determination (R^2).

Parameter	*CEI*		*TDI_{30}*		*SS_{max}*		*ASS*		*CS*	
	r	R^2	r	R^2	R	R^2	r	R^2	r	R^2
G/S	0.62	0.39	-0.88	0.78	0.97	0.93	0.98	0.96	-0.93	0.87
n	0.69	0.47	-0.92	0.84	0.98	0.97	0.96	0.92	-0.96	0.92
CA Ratio	-0.69	0.48	0.92	0.85	-0.99	0.97	-0.96	0.91	0.96	0.92
FAc Ratio	-0.53	0.28	0.82	0.68	-0.93	0.87	-1.00	0.99	0.88	0.78
FAf Ratio	-0.62	0.39	0.88	0.78	-0.97	0.93	-0.98	0.96	0.93	0.87
CAr	0.64	0.41	-0.89	0.80	0.97	0.95	0.97	0.95	-0.94	0.88
C/F	0.72	0.52	-0.94	0.88	0.99	0.98	0.94	0.89	-0.97	0.94
FArmf	0.62	0.38	-0.88	0.77	0.96	0.93	0.98	0.96	-0.93	0.86

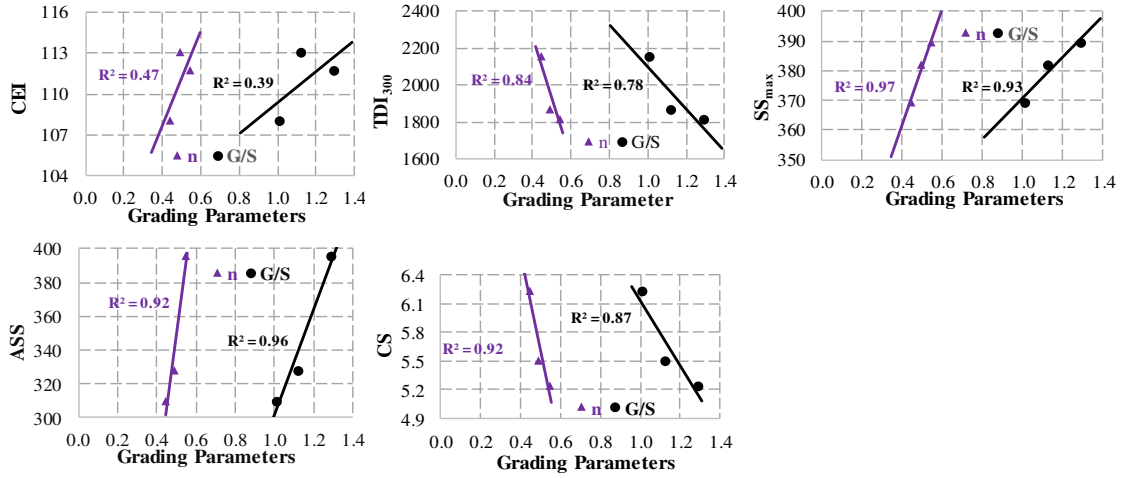

Figure 5. Gradation and Compactability Parameters Correlations.

Figure 5 show the graphical illustration of the correlation trends between the aggregate gradation parameters (i.e., G/S and n) and compactability parameters. The SS_{max} and ASS compactability parameters show a positive correlation with both the G/S and n, indicating that for the gradation structures investigated, the coarser gradation exhibits higher shear resistance. On the other hand, the TDI_{300}, and CS parameters show a negative correlation with the G/S and n parameters, but also indicating the coarser the gradation, the more difficult it is to compact. The

CEI showed a relatively weaker positive correlation. This could be due to the fact that the CEI is determined in the early stage of the compaction process (i.e., from 8th gyration to 92% compaction), while the HMA mix is still in a loose state. Hence, influence of the aggregate gradation is still insignificant. With respect to the slope (rate of change), relationships with the *n* parameter exhibits a steeper slope than with the G/S parameter. This is primarily due to the differences in the range of the grading parameter values (i.e., *n* values range from 0.44 for finer gradation to 0.55 for coarser gradation, whereas G/S values range from 1.01 for finer gradation to 1.29 for coarser gradation.

The correlation trends for the traditional and the revised Bailey ratios are presented in Figure 6 and Figure 7, respectively. Contrary to the gradation parameters (*n* and G/S), the traditional Bailey ratios exhibited opposite correlation trends. This was expected because the traditional Bailey ratios were formulated in an inverse form (i.e. fine/coarse). For the revised rational Bailey ratios, as expected the correlation trends are similar to the gradation parameters (G/S and *n*), but opposite with the traditional Bailey ratios. Similar to the gradation parameters, the rate of change of the compactability parameters structure is determined by the range of the Bailey ratios.

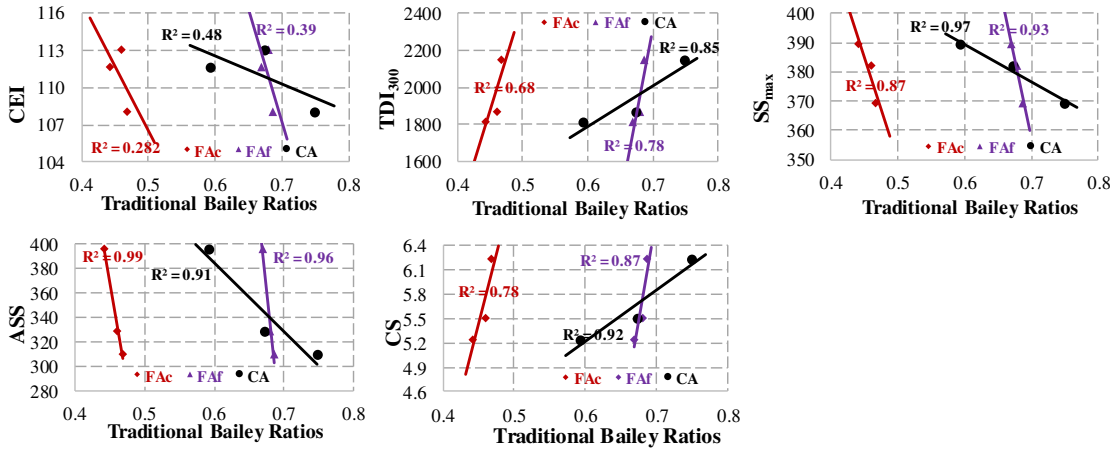

Figure 6. Traditional Bailey Ratios and Compactability Parameters Correlations

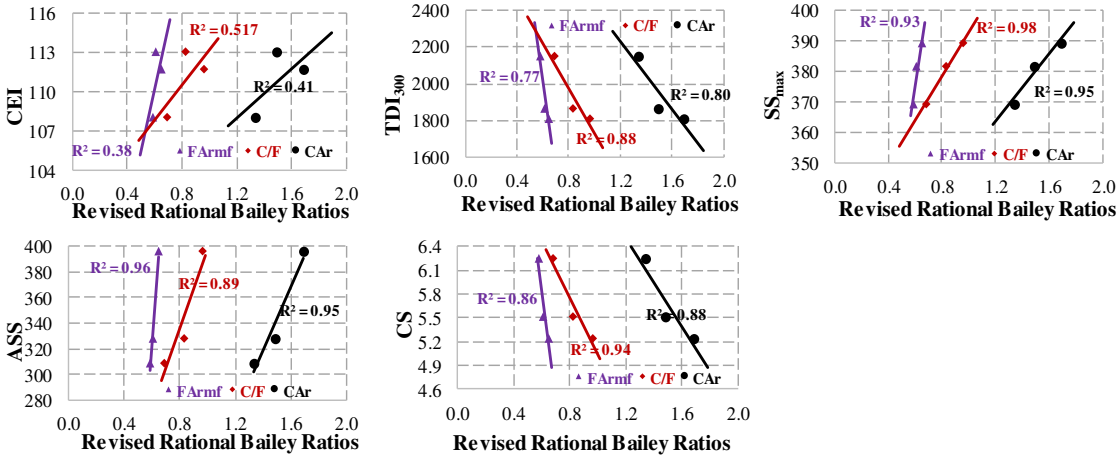

Figure 7. Rational Bailey Ratios and Compactability Parameters Correlations

CONCLUSION AND RECOMMENDATIONS

This paper investigated the influence of aggregate packing characteristics on HMA compactability. Two gradation parameters (G/S and *n*), three traditional (CA, FA*c* and FA_f) and revised rational (CA_r, C/F and FA_{rmf}) Bailey ratios were correlated with five different HMA mix compactability parameters (CEI, TDI_{300}, SS_{max}, ASS and CS). Based on the results and discussions contained in this paper, the following conclusions are drawn and recommendations made.

- The gradation parameters and the Bailey ratios showed a strong correlation with parameters TDI_{300}, SS_{max}, ASS and CS of HMA compactability ($r > |0.88|$). However, correlations for CEI were found to be relatively weaker to medium (r ranging from |0.53| to |0.72|). This could be due to the fact that the CEI is determined in the early stage of the compaction process (i.e., from 8th gyration to 92% compaction), while the HMA mix is still in a loose state at which the influence of the aggregate gradation structure is not prominent;
- A new traffic densification index (TDI_{300}) proposed in the study showed a good correlation (r ranging from |0.93| to |0.99|) with the packing parameters and
- Additionally, two shear stress-based HMA compactability parameters (SS_{max} and ASS) proposed in this study were also found to correlate very well with the aggregate gradation parameters and the Bailey ratios.

Overall, this study demonstrated that the aggregate gradation structure, play a significant role in the compactability of an HMA mix, and this should be considered carefully when selecting a combination of individual aggregate fractions during the HMA design and production. The findings of this study suggest that for a specific gradation structure, the coarser the gradation structure, the higher the energy required to compact the resulting HMA.

As study focused on coarse gradation structure, future work should include more HMA mixes and other types of gradation structures to validate the findings. The influence of other attributes such as aggregate type and shape properties, also need be investigated. Although limited to three aggregate gradations, the study demonstrated that aggregate gradation parameters and Bailey ratios that can easily be computed from the basic gradation curve, may be very useful in terms of predicting the compactability of HMA mixes, without the need for the additional laboratory or field testing. Furthermore, the aggregate gradation parameters and Bailey ratios have the potential to be used as input parameters when developing models to simulate HMA compaction.

ACKNOWLEDGMENTS

The authors would like to acknowledge the South African Council for Scientific and Industrial Research (CSIR) for funding and supporting this study. Special thanks also go to all those who assisted during the course of this study.

REFERENCES

Anochie-Boateng, J., Denneman, E., O'Connell, J. and Ventura, D. (2010). Test Protocols for determining properties of asphalt materials for SAPDM. *TECHNICAL REPORT No: CSIR/BE/IE/IR/2010/0001/B*, CSIR, Pretoria.

Alshamsi, KS. (2006). Development of mix design methodology for asphalt mixtures with analytically formulated aggregate structures. *PhD Thesis. Louisiana State University and*

Agricultural and Mechanical College, USA.
Asphalt Institute. (1996). Superpave Mix Design. *Superpave Series No. 2 (SP-2),*USA
Awed, A., Kassel, E., Masad, E. and Little, D. (2015). Method for Predicting the Laboratory Compaction Behavior of Asphalt Mixtures. *J. Materials in Civil Engineering*. Vol. 27 (11).
Bahia, HU., Firemen, TOP., Peterson, P.A., Russell, J.W. and Penult, B. (1998). Optimization of constructability and resistance of traffic: a new design approach for HMA using the superpave compactor. *J. Association of Asphalt Paving Technologists*.Vol. 67, pp. 189-232.
Chang, K.G. and Meegoda, J.N. (1997). Micromechanical simulation of hot mix asphalt. *J. Engineering Mechanics*. Vol. 123, pp. 495-503.
COLTO. (1998). Standard Specifications for Road and Bridge Works for State Authorities. SAICE, Midrand, South Africa.
Fuller, W.B. and Thompson, S.E. (1907). *The laws of proportioning concrete*. *American Society of Civil Engineers*. Vol. LIX (2), pp. 67-143.
Horak, E., Sebaaly, H., Maina, J. and Varma, S. (2017). Rational Bailey ratios and dominant aggregate size range porosity with rutting and mixture strength parameters. *36th Southern African Transport Conference*. July 2017, Pretoria.
Horak and Cromhout (2018) Permeability Potential of Asphalt Mixes via Binary Aggregate Packing Principles Applied to Bailey Method Ratios and Porosity Principles. *Proceedings of the 2018 SARF/IRF/PIARC,* October 2018, Durban.
Kutay, M.E., Varma, S. and Jamrah, A. 2015. A micromechanical model to create digital microstructures of asphalt mastics and crumb rubber-modified binders. *International Journal of Pavement Engineering*, Vol. 18 (9), pp. 754-764.
Masad, E., Muhunthan, B., Shashidhar, N and Harman, T. (1999). Quantifying laboratory compaction effects on the internal structure of asphalt concrete. *Transportation Research Record* No. 1681, pp. 179-185.
Micaelo, R., Azevedo, M.C., Ribeiro, J. and Azevedo, N. (2009). Discrete element simulation modelling of field asphalt compaction. *Sixth International Conference on Maintenance and Rehabilitation of Pavements and Technological Control (MAIREPAV6).* Torino, Italy.
Olard F., (2015).*GB5:* Innovative design of High-Performance Asphalt Mixes for Long-Life and Cost –effective Pavements by Optimizing Aggregates and using SBS Modified Bitumen. *Proceedings of the Conference on Asphalt Pavements in Southern African (CAPSA).* August 2015 Sun City, South Africa.
SABITA. (2016). Manual 35/TRH 8: Design and use of asphalt in road pavements.
Sanchez-Leal, F.L. (2007). Gradation chart for asphalt mixes: Development. *J. material in civil engineering*. Vol. 19 9 (2), pp. 185-197.
SABS. (2011a). SANS 3001-AS11: Determination of the maximum void-less density of asphalt mixes and the quantity of binder absorbed by the aggregates.
SABS. (2011b). SANS 3001-AS10: Determination of bulk density and void content of compacted asphalt.
SABS. (2014). SANS 3001-AG1: Particle size analysis of aggregates by sieving.
SABS. (2016). SANS 4001-BT1: Part BT1: Penetration grade bitumen.
Shen, S. and Yu, H. (2011*). Characterize packing of aggregate particles for paving materials: Particle size impact*. *Construction and Building Materials*. Vol. 25.
Vavrik, W.R., Huber, G., Pine, W.J., Carpenter, S.H., and Bailey, R. (2002). Bailey method for gradation selection in hot-mix asphalt mixture design. *Transportation Research E-Circular, Number E-C044*, Washington D.C., USA.

Verhaeghe, B., Myburgh, P.A., and Denneman, E. (2007). Asphalt rutting and its prevention. *Presented at the 9th Conference on Asphalt Pavements for Southern Africa*. September 2007, Gaborone.

Walubita, L. F.; Jamison, B.; Alvarez, A. E., X. Hu, and C. Mushota (2012). Air void characterization of hot mix asphalt gyratory laboratory-molded samples and field cores using X-ray computed tomography (X-ray CT)". *J. South African Institution of Civil Engineering*, Vol 54 (2), pp. 22-31.

Walubita, L.F., A. N.M. Faruk, J. Zhang, X. Hu, & S. I. Lee (2016). The Hamburg Rutting Test – Effects of HMA Sample Sitting Time and Test Temperature Variation. *J. Construction and Building Materials*, Vol. 108 22-28.

Wang, J.N., Kennedy, T.W. and Mcgennis, T.W. (2000). Volumetric and Mechanical Performance Properties of Superpave Mixtures. *J. Materials in Civil Engineering*. Vol. 12(3).

Xu, R., Yand, X.H., Yin, A.Y., Yang, S.F., and Ye, Y. (2010). Three-Dimensional Aggregate Generation and Packing Algorithm for Modeling Asphalt Mixture with Graded Aggregates. *J. Mechanics*. Vol. 26 (2), pp. 165-171.

Investigation into Flat and Elongated Particles Ratio for Asphalt Mix Design Using a Modern Laser Technique

J. Anochie-Boateng, Ph.D., M.ASCE[1]; and G. Mvelase[2]

[1]Council for Scientific and Industrial Research (CSIR), PO Box 395, Pretoria 0001, South Africa. E-mail: janochieboateng@csir.co.za
[2]Council for Scientific and Industrial Research (CSIR), PO Box 395, Pretoria 0001, South Africa. E-mail: gmvelase@csir.co.za

ABSTRACT

Flat and elongated particle ratio is a shape characteristic for coarse aggregates used in pavements. The ASTM D 4791 is the standard test method to determine flat and elongated coarse aggregate particles in asphalt mixes. However, this method is subjective, making it less reliable to accurate measurements. The objective of this study was to investigate three flat and elongated particles ratios (FERs): 2:1, 3:1, and 5:1 using a modern 3-D laser scanning technique and compare results with ASTM D 4791. Based on the ASTM D4791, the Superpave specification allows for a maximum of 10% coarse aggregates to have FER of 5:1 in asphalt mixes. Eight aggregate materials used for road construction in South Africa were investigated. The results indicate that three crushed stones would be rejected by the Superpave specification whereas all eight crushed stones could meet the specification based on the results from the 3-D laser scanning method.

INTRODUCTION

The traditional ASTM D4791 test method used to determine flat and elongated coarse aggregate particles in asphalt mixes is less reliable to accurate measurements as the entire procedure is highly subjective hence liable to human errors. There is a general interest worldwide in employing imaging and automated techniques to characterize the shapes of aggregates used in pavements. The main advantage these techniques is the ability to capture three-dimensional (3-D) information of aggregate shapes, hence allowing for a more accurate and precise measurements.

Aggregate shapes govern the deformation and strength characteristics of asphalt mixes. Modern asphalt mix design methods emphasize on aggregate shape properties that improve performance of the pavement. For instance, equal-dimensional aggregate particles are generally preferred over flat and elongated aggregates in the asphalt mix. The propensity of flat and elongated particles to lock up or break during compaction may lead into difficulties in achieving air voids requirements in asphalt mixes. Accordingly, various mix design specifications limit the amount of flat and elongated particles in the asphalt mix.

Several studies have shown that aggregate shape parameters measured using automated and advanced imaging techniques are more accurate when compared with standard methods (Brian et al. 2005, Rao et al. 2001, Anochie-Boateng et al, 2012, Prowell and Weingart, 1999.). Marez and Zhou (1999) underlined advantages of digital image system as reliable, increased testing and quicker process control adjustment to reduce off-specification material and less subjective than the traditional manual measurements. Most of these techniques make use of the aggregate particle dimensions (length, width and thickness) as well as area and volume to compute indices describing aggregate shape.